

BULLETIN
DE
L'ACADÉMIE POLONAISE
DES SCIENCES

Rédacteur en chef
K. KURATOWSKI

Rédacteur en chef suppléant
S. KULCZYŃSKI

CLASSE TROISIÈME

Rédacteur de la Série
L. INFELD

Comité de Rédaction de la Série
K. BORSUK, S. LESZCZYCKI, J. SAMSONOWICZ, M. ŚMIAŁOWSKI

VOLUME I
NUMÉRO 5

VARSOVIE 1953

PRINTED IN POLAND

PAŃSTWOWE WYDAWNICTWO NAUKOWE — WARSZAWA 1953

Nakład 1.150 egz. + 50 odb.	Rękopis dostarczono 25. VIII. 1953
Ark. wyd. 3, druk. 3	Podpisano do druku 30. X. 1953
Papier bezdrzewny sat. 70 g, III kl.	Druk ukończono 12. XI. 1953
Format 70×100 cm	Zam. prod. 363/53 Cena zł 5.—

KRAKOWSKA DRUKARNIA NAUKOWA, KRAKÓW UL. CZAPSKICH 4

The Solution of a Certain Problem on Graphs of P. Turan

by

K. ZARANKIEWICZ

Communicated by K. KURATOWSKI at the meeting of February 23, 1953

The problem is to define the smallest number of intersection points of the sides of a certain graph, defined in the Theorem. This Theorem gives not only the solution of Turan's problem but also the minimum number of regions into which the graph cuts the plane.

Theorem. *If*

(α) *in the Euclidean plane two sets of points, A and B, are given, A consisting of p points $a_1, a_2, a_3, \dots, a_p$, and B consisting of q points $b_1, b_2, b_3, \dots, b_q$ (p and q are natural numbers);*

(β) *for each pair of points a_i, b_j , where $i = 1, 2, 3, \dots, p, j = 1, 2, 3, \dots, q$, there exists a simple arc, lying in the plane and having points a_i, b_j as its end points;*

(γ) *the arcs lie in such a way that no three arcs have an interior point (i. e. a point that is not an end point) in common;*

(δ) $K(p, q)$ *denotes the smallest number of intersection points between the arcs;*

(ϵ) $L(p, q)$ *denotes the smallest number of regions into which the plane is cut by all the simple arcs;*

then the following formulas hold:

$$K(2k, 2n) = (k^2 - k)(n^2 - n),$$

$$K(2k, 2n + 1) = (k^2 - k)n^2,$$

$$K(2k + 1, 2n + 1) = k^2 n^2.$$

$$L(2k, 2n) = (k^2 - k)(n^2 - n) + 4nk - 2(n + k) + 2,$$

$$L(2k, 2n + 1) = (k^2 - k)n^2 + 4nk - 2n + 1,$$

$$L(2k + 1, 2n + 1) = n^2 k^2 + 4nk + 1.$$

The proof, based on the theorems contained in the papers of K. Zarankiewicz, „Über eine topologische Eigenschaft der Ebene“, Fund. Math. 11 (1928), 19—26; K. Kuratowski et K. Zarankiewicz, „Sur un problème concernant les coupures des régions par des continus“, Fund. Math. 39 (1953), 15—24 and S. Straszewicz, „Über die Zerschneidung der Ebene durch

abgeschlossene Mengen“, Fund. Math. 7 (1925), 159—187, will be published in Fund. Math. 41.

For each pair of natural numbers p, q , it is possible to construct a minimum graph in which the number of intersection points of all its sides is expressed exactly by the formulas of the Theorem. This means that $K(p, q)$ and $L(p, q)$ have been attained.

Minimum graph. If $p = 2k$, set A consists of the points on the x -axis whose abscissas are: $-k, -(k-1), \dots, -2, -1, +1, +2, \dots, +k$; if $p = 2k + 1$, set A consists of the points on the x -axis whose abscissas are $-k, -(k-1), \dots, -2, -1, +1, +2, \dots, +k, +k+1$; if $q = 2n$, set B consists of the points on the y -axis whose ordinates are $-n, -(n-1), \dots, -2, -1, +1, +2, \dots, +n$; if $q = 2n + 1$, set B consists of the points on the y -axis whose ordinates are $-n, -(n-1), \dots, -2, -1, +1, +2, \dots, +n, +n+1$. By joining each point of set A with each point of set B by a line-segment, we obtain a minimum graph, in which the number of intersection points of the sides is expressed exactly by the formulas of the Theorem, which can easily be checked.

Let us note, by the way, that assumption (γ) is essential. If we reject it, $K(p, q) = 1$ for any pair of numbers $p > 3$ and $q > 3$. Indeed, taking any point x of the plane, we can join it by means of simple arcs with each of the points of the set $A + B$ in such a manner that these arcs will have only one point in common, namely point x . Then assumption (β) is observed, and the number of intersection points of all the arcs is 1.

Note. Let us observe that the Theorem will remain true when, instead of simple arcs joining points a_i and b_j , we take any continua M_{ij} , joining those points, provided $M_{ij} - a_j - b_j$ is a connected set.

Occultation d'une Étoile fondamentale par le II Satellite de Jupiter le 20 Novembre 1952

(Annonce)

par

T. BANACHIEWICZ

Présenté à la séance du 17 Novembre 1952

Le 20 Novembre 1952 l'étoile fondamentale σ Arietis, de 5.5 grandeur, Sp. B5, sera en conjonction, accompagnée de l'occultation, avec Europa, le second satellite de Jupiter.

En empruntant la position de l'étoile (*) aux Apparent Places of Fundamental Stars, 1952, Londres, et la position de Jupiter (J) au Nautical Almanac, 1952, Londres, on a pour 1952 Nov. 20.12 T. U.

$$\begin{aligned} \alpha_* + 2^{\text{h}} 48^{\text{m}} 55^{\text{s}}.139 \quad \delta_* &= +14^{\circ} 53' 33''.92 \\ \alpha_J &= 2^{\text{h}} 49^{\text{m}} 6^{\text{s}}.327 \quad \delta_J &= +14^{\circ} 54' 37''.06 \end{aligned}$$

donc, pour ce moment

$$\begin{aligned} \alpha_J - \alpha_* &= +11^{\text{s}}.188 = +162''.17 \quad (\text{en grand cercle}) \\ \delta_J - \delta_* &= +63''.14 \end{aligned}$$

Dans les coordonnées de l'étoile on n'a pas tenu compte des termes à courte période, puisqu'ils sont négligés dans l'éphéméride de la planète. De pareilles différences des coordonnées pour les instants 1952 Nov. 20.10 et Nov. 20.14 T. U. sont données dans le Tableau (I) ci-dessous.

Les coordonnées polaires du Satellite ont été tirées des Tables de Sampson (Tables of the four great satellites of Jupiter, 1910). Pour le temps d'aberration de Jupiter on a admis $33.24 = 0.0232$ d'après la Connaissance des Temps 1952, p. 557, et l'on a obtenu pour Europa pour les instants 1952 Nov. 20.10, 20.12 et 20.14 T. U., équivalents, en tenant compte d'aberration, aux instants Nov. 19.5768, 19.5968 et 19.6168 T. M. G. (en négligeant ici et de même dans tout le calcul la différence des temps d'aberration pour la planète et le Satellite, ainsi que la nutation) les coordonnées suivantes, rapportées au plan de Jupiter de 1900.0 et au point vernal de la date

Tableau I

1952	Nov. 20.10	Nov. 20.12	Nov. 20.14
l	⁰ 271.896	⁰ 273.930	⁰ 275.966
b	⁰ -2.563	⁰ -2.466	⁰ -2.367
r/a	0.99848	0.99815	0.99782

Pour en déterminer les coordonnées géocentriques différentielles du Satellite on a employé les deux méthodes suivantes:

1. Le procédé exposé dans notre travail sur le calcul des positions apparentes des satellites, *Astr. Nachr.* **191** (1912), 7 (4567), p. 121. À cet effet on a mis maintenant les formules de ce travail en forme cracovienne. On y calcule les positions de Jupiter rapportées au plan de référence des Tables de Sampson, les coordonnées polaires jovicentriques et géocentriques du Satellite par rapport à cette position sphérique, et, après avoir rapporté les angles de position à la direction vers le pôle Nord, on finit par calculer les coordonnées relatives $\Delta\alpha \cos \delta$ et $\Delta\delta$ (Sat.—Jup.) en négligeant les termes du 3-me ordre.

2. Dans la seconde méthode, un peu plus directe, on emploie les formules de Polygonométrie sphérique (*Roczn. Astr. Obs. Krak., Suppl. Int.* **19** (1948)) et les „coefficients de précession“, publiés annuellement dans le *Roczn. Astr. Obs. Krak.*, pour passer des longitudes l (après y avoir retranché la précession depuis 1900.0 jusqu'à l'époque) et des latitudes b aux coordonnées jovicentriques équatoriales α_s, δ_s , du Satellite de l'époque et l'on finit par l'application des formules rigoureuses de la théorie de paralaxe convenablement adaptées au problème en question.

De cette façon nous avons obtenu le Tableau suivant des coordonnées apparentes relatives de Jupiter et d'Europa (S) pour les trois époques ci-dessus

Tableau II

1952	Nov. 20.10		Nov. 20.12		Nov. 20.14	
	$\Delta\alpha$	$\Delta\delta$	$\Delta\alpha$	$\Delta\delta$	$\Delta\alpha$	$\Delta\delta$
J — * =	+ 177.04	+ 65.68	+ 167.82	+ 63.14	+ 158.60	+ 60.58
(I) S — J =	- 163.54	- 62.38	- 168.94	- 63.62	- 174.12	- 64.78
S — * =	+ 13.50	+ 3.30	- 1.12	- 0.48	- 15.52	- 4.20
ou, en grand cercle ($\Delta\alpha \cos \delta$ et $\Delta\delta$)						
S — * =	+ 13.05	+ 3.30	- 1.08	- 0.48	- 15.00	- 4.20

Il en suit pour le moment de la conjonction géocentrique en ascension droite

1952 Nov. 20 2^h 50^m 6 T. U.

$$\Delta\delta (\text{Europa} - \sigma \text{ Arietis}) = - 0''.19$$

le diamètre apparent du Satellite étant d'environ 1''. La vitesse relative du Satellite par rapport à l'étoile est de 0''.504 par minute.

Le circonstances de la conjonction peuvent être évidemment affectées par les erreurs des positions de l'Étoile (appartenant au FK3), de Jupiter et des Tables du Satellite. Vu la grande rareté du phénomène (une occultation d'une étoile fondamentale par un des grands satellites de Jupiter dans une place donnée de la Terre n'ayant lieu probablement qu'une fois par plus de 1000 ans) l'Académie Polonaise des Sciences l'a annoncé par télégraphe aux centrales astronomiques de Poulkovo, Copenhague et Cambridge, Mass.

An Application of a New Approximation Method to Quantum Calculations in the Meson Theory of Nuclear Forces

by

J. WERLE

Communicated by L. INFELD at the meeting of November 17, 1952

The method of successive approximations [1], the general scheme of which was given in a previous communication [2], can also be applied in the frame-work of the quantum theory. This we shall show in detail for the case of a pseudoscalar meson field. From the usual action function, the following equations for the meson field and ψ function can be deduced:

$$(1) \quad (\square - \mu^2)\varphi = -4\pi g \psi^* \varrho_2 \psi + 4\pi \frac{f}{\mu} (\psi^* \sigma^\nu \psi)_{,\nu}$$

$$(2) \quad i \frac{\partial \psi}{\partial t} = \left\{ -i \alpha^k \frac{\partial}{\partial x^k} + \varrho_3 M - g \varrho_3 \varphi - \frac{f}{\mu} \sigma^\nu \varphi_{,\nu} \right\} \psi$$

where we use the usual notations:

φ — the pseudoscalar meson field

ψ — the wave function of the nucleons (ψ^* — its Hermitian adjoint).

$\varrho_k, \sigma^\nu, \alpha^\nu$ — Dirac matrices in the usual form ($\alpha^4 = i, \sigma^4 = i \varrho_1$) $c = 1$, $\hbar = 1$.

Let us consider the field produced by a transition of a nucleon denoted by (1) from a state described by the wave function ψ to another state described by ψ' . For convenience we write the expressions referring to the sources on the right side of (1) in the integral form:

$$(3) \quad \psi^* \varrho_2^{(1)} \psi = \int \psi'^* (\vec{x}_{(1)} t) \varrho_2^{(1)} \delta(\vec{x}_{(1)} - \vec{x}) \psi(\vec{x}_{(1)} t) d_3 x_{(1)}.$$

$$(4) \quad \frac{\partial}{\partial x^\nu} (\psi^* \sigma^\nu_{(1)} \psi) = \frac{\partial}{\partial x^\nu} \int \psi'^* (\vec{x}_{(1)} t) \sigma^\nu_{(1)} \delta(\vec{x}_{(1)} - \vec{x}) \psi(\vec{x}_{(1)} t) d_3 x_{(1)}.$$

As for space differentiations in this last expression, we can place them directly under the integral sign, operating on the variables \vec{x} in the δ function. With regard to time derivatives we assume quite generally that both ψ and $\dot{\psi}$ satisfy the same equation of «motion» for one particle (it does not need to be of the same form as (2)):

$$(5) \quad i \frac{\partial \psi(1)}{\partial t} = H^{(1)} \psi(1)$$

Thus we can replace in the well-known manner all the time derivatives by the commutators and obtain:

$$(6) \quad \begin{aligned} & \frac{\partial}{\partial x^\nu} (\dot{\psi}^* \sigma_{(1)}^\nu \psi) = \\ & = \int \dot{\psi}^*(\vec{x}_1 t) \left\{ \sigma_{(1)}^k \frac{\partial \delta(\vec{x}_{(1)} - \vec{x})}{\partial x^k} + i [H^{(1)}, \varrho_{(1)}^1 \delta(\vec{x}_{(1)} - \vec{x})] \right\} \psi(x_{(1)} t) d_3 x_{(1)}. \end{aligned}$$

In order to compute the commutator we can take the usual form (2) for the $H^{(1)}$

$$(7) \quad H^{(1)} = -i \alpha_{(1)}^k \frac{\partial}{\partial x_{(1)}^k} + \varrho_{(1)}^3 M - g \varrho_{(1)}^2 \varphi - \frac{f}{\mu} \sigma_{(1)}^\nu \varphi_{,\nu}$$

It follows that

$$(8) \quad \begin{aligned} & i \left[-i \alpha_{(1)}^k \frac{\partial}{\partial x_{(1)}^k} + M_1 \varrho_{(1)}^3 + g \varrho_{(1)}^2 \varphi - \frac{f}{\mu} \sigma_{(1)}^\nu \varphi_{,\nu} - \varrho_{(1)}^1 \delta(\vec{x}_{(1)} - \vec{x}) \right] = \\ & = -\sigma_{(1)}^k \frac{\partial \delta(\vec{r}_{(1)})}{\partial x^k} - 2 M_1 \varrho_{(1)}^3 \delta(\vec{r}_{(1)}) - 2 g \varrho_{(1)}^2 \delta(\vec{r}_{(1)}) \varphi. \end{aligned}$$

The first term exactly cancels the expressions obtained from space differentiations. There remains

$$(9) \quad -\frac{2M}{\mu} f \int \dot{\psi}^* \varrho_{(1)}^3 \delta(\vec{r}_{(1)}) \psi d_3 x_{(1)} - \frac{2gf}{\mu} \int \dot{\psi}^* \varrho_{(1)}^3 \delta(\vec{r}_{(1)}) \psi \varphi d_3 x_{(1)}.$$

The first expression has the same form as for pure pseudoscalar coupling, the second contains a meson field but it appears only when both the f and g coupling constants are different from zero.

In the following we shall restrict ourselves to the pure pseudoscalar sources. The form of (5) shall not be specified as yet.

We have now:

$$(10) \quad (\square - \mu^2) \varphi = -4\pi g \int \dot{\psi}^*(1) \varrho_{(1)}^3 \delta(\vec{r}_{(1)}) \psi(1) d_3 x_{(1)}.$$

The integral operator on the right side, acting on the δ function, commutes with the Laplacian operator Δ . Therefore the general approximation scheme given in a previous communication [2] can be applied to the present quantum mechanical case too. Putting as before $\varphi = \Sigma_2 \varphi$ we get:

$$(11) \quad {}_0\varphi = g \int \dot{\psi}(1) \varrho_2^{(1)} \frac{e^{-\mu r_{(1)}}}{r_{(1)}} \psi(1) d_3 x_{(1)}.$$

$$(12) \quad {}_2\varphi = g \int \dot{\psi}^*(1) \left[H^{(1)}, \left[H^{(1)}, \varrho_2^{(1)} \frac{e^{-\mu r_{(1)}}}{2\mu} \right] \right] \psi(1) d_3 x_{(1)} \dots$$

The above result for φ makes possible an easy construction of the interaction operator between two nucleons. Let us compute a matrix element of this operator corresponding to the following transition

$$(13) \quad \begin{aligned} \psi(1) &\rightarrow \dot{\psi}(1) \\ \psi(2) &\rightarrow \dot{\psi}(2). \end{aligned}$$

This element, which is closely related to the interaction energy of two given sources, can be formed in an analogous way to that used in electrostatics (compare C. Møller [3]). The source density of the second particle taken in the same form as in (10) must be multiplied by the field φ , created by the first particle, and the result must be integrated over the whole space. Thus we obtain for the required matrix element:

$$(14) \quad -g \int \dot{\psi}^*(2) \varrho_2^{(2)} \psi(2) \varphi(2) d_3 x_{(2)} = \int \dot{\psi}^*(1) \cdot \dot{\psi}^*(2) V(2 \leftarrow 1) \psi(1) \psi(2) d_3 x_{(1)} d_3 x_{(2)}.$$

The quantity $V(2 \leftarrow 1)$ defined by this equation can be considered as representing the action of the first particle upon the second one. Hence it follows that:

$$(15) \quad V(2 \leftarrow 1) = -g^2 \left\{ \varrho_2^{(1)} \varrho_2^{(2)} \frac{e^{-\mu r_{12}}}{r_{12}} + \frac{\varrho_2^{(2)}}{2\mu} [H^{(1)}, [H^{(1)}, \varrho_2^{(1)} e^{-\mu r_{12}}]] + \dots \right\}.$$

Most authors used the momentum representation for relativistic quantum calculations. Therefore, in order to compare our results with those of other authors, we compute the matrix element of $V(2 \leftarrow 1)$ assuming the simplest possible form for the equation of »motion«. Namely we take for $H^{(1)}$ the free particle Hamiltonian and compute the matrix element corresponding to the following transition:

particle (1) from a state of definite momentum and energy (\vec{p}_1, E_1) to another such state (\vec{p}_1', E_1') ,

particle (2) from (\vec{p}_2, E_2) to (\vec{p}_2', E_2') .

In consequence the ψ 's are now eigenfunctions of the operators

$$(16) \quad H^{(1)} = -i a_{(1)}^k \frac{\partial}{\partial x_{(1)}^k} + \varrho_3^{(1)} M$$

e. g.

$$(17) \quad \psi(1) = \frac{1}{(2\pi)^{3/2}} u(\vec{p}_1, \vec{E}_1) e^{i(\vec{p}_1, \vec{x}_{(1)} - E_1 t)}$$

where $u(\vec{p}_1 E_1)$ denotes a constant spinor, satisfying

$$(18) \quad (\alpha_{(1)}^k p_{(1)}^k + \varrho_{(1)}^{(1)} M_1) u(\vec{p}_1 E_1) = E_1 u(\vec{p}_1 E_1).$$

Finally, we get for the required matrix element

$$(19) \quad -g^2/2\pi^2 u^{*(1)}(1) \varrho_2^{(1)} u(1) u^{*(1)}(2) \varrho_2^{(2)} u(2) \left\{ \frac{1}{(\vec{p}_1 - \vec{p}_1') + \mu^2} + \frac{(E_1' - E_1)^2}{\{(\vec{p}_1 - \vec{p}_1') + \mu^2\}^2} + \right. \\ \left. + \dots \right\} e^{i(E_1 t + E_2 t' - E_1 t - E_2 t')} \delta(\vec{p}_1 + \vec{p}_2 - \vec{p}_1' - \vec{p}_2')$$

The δ function at the end of this expression means that only these transitions give matrix elements different from zero for which momentum is conserved $\vec{p}_1 + \vec{p}_2 = \vec{p}_1' + \vec{p}_2'$.

Our expansion is convergent for all \vec{p}_1 and \vec{p}_1' if we exclude transitions accompanied with change of energy sign. Then we can sum up the expansion (19) and obtain (omitting the time factor):

$$(20) \quad -\frac{g^2}{2\pi^2} u^{*(1)}(1) u^{*(2)}(2) \frac{\varrho_2^{(1)} \varrho_2^{(2)}}{(\vec{p}_1 - \vec{p}_1')^2 + \mu^2 - (E_1' - E_1)^2} u(1) u(2) \delta(\vec{p}_1 + \vec{p}_2 - \vec{p}_1' - \vec{p}_2').$$

This is just the usual form which can be obtained for instance from the second order perturbation treatment of the meson field.

It is easy to see that the method presented is not restricted to the above simplified case. It can be used also in these cases when the equation of motion is assumed to be given but has a more complicated form (e. g. can contain the static interaction operator as a first approximation). Finally, if we use the many-time formalism similar to that of Dirac-Fock-Podolski we can use this method for an iterative solution of simultaneous equations of field and motion. We shall discuss these problems in detail on another occasion.

The author is very much indebted to prof. L. Infeld for many interesting discussions.

Institute of Theoretical Physics, University of Warsaw

REFERENCES

- [1] Einstein A., Infeld L., Hoffmann B., Ann. Math. **39** (1938), 65.
— Infeld L., Phys. Rev. **53** (1938), 836.
- [2] Werle J., Bull. Ac. Pol. Sc. **1** (1953), 23.
- [3] Møller C., Z. f. Phys. **70** (1931), 786, Ann. Phys. **14** (1932), 531.

An Example of V_1^0 -Decay Recorded in Photographic Emulsion

by

M. DANYSZ

Communicated by A. SOŁTAN at the meeting of February 23, 1953

An event which may be regarded as an example of V_1^0 decay, was recently observed in this laboratory. It was recorded on a G5 Ilford plate with emulsion 600μ thick. The plate was exposed to cosmic radiation at high altitude.

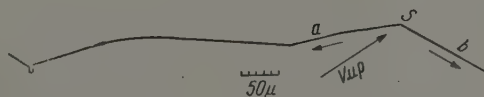


Fig. 1

Two tracks, marked a and b , start from point S , no trace of recoil being visible. They form an angle of 128° . Track a , 680μ long, ends in the emulsion with a small one-prong star (one black track and a short recoil). Both scattering and grain-density indicate that this track is caused by a light particle, the mass of which is certainly less than $1000m_e$ and probably of the order of a few hundred electron masses. Track b , after 13000μ , runs into the glass. The grain-density measurements on its first and second half give respectively:

$$\begin{aligned} g_1 &= (33.0 \pm 0.34) \text{ grains per } 50\mu \\ g_2 &= (34.2 \pm 0.34) \text{ " " " "} \end{aligned}$$

As there is a significant increase in grain-density, we assume that particle b starts from point S . The evaluation of the mass of particle b , based on grain-density and multiple scattering measurements*) using the

) Grain density was normalized on high-energy electron tracks of electron pairs $g^ = g/g_{p1}$ (g_{p1} — grain-density on the relativistic plateau) [1]. Errors on g and the scattering parameter \bar{a} were estimated according to the convention used by Daniel et al. [2].

calibration curve, as determined by [1] gives:

$$m_b = (1690 \pm 140)m_e.$$

Thus it seems reasonable to assume that a is a π -meson track and b — a proton-track.

This simultaneous emission of a proton and a π -meson without any visible recoil, suggests that the whole event may be considered as an example of the decay in flight of a V_1^0 -particle. Closer analysis lends strong support to this view.

The angle between the direction of the emission of the assumed decay products in the C -system and the direction of the flight of the parent particle is about 20° . The trajectory of the assumed parent particle, as calculated from the momentum diagram, enters the emulsion about 7 millimeters ahead of event S . The plate was scanned in this direction. We found no event which might be regarded as constituting the possible source of a V_1^0 -particle in the corresponding volume of emulsion. This result is in conformity with the estimated life-time of a V_1^0 -particle. The Q -value of decay, as calculated from the angle of emission and the momenta of the decay products, yields (35.5 ± 2) Mev. This agrees well with the estimate derived from cloud chamber data: (36 ± 3) Mev.

Taking into account all the features of event S , and especially the value of Q , we are drawn to the conclusion that this event does in fact constitute the decay in flight of a V_1^0 -particle. Should this conclusion be correct, the event may be regarded as direct evidence of the emission of a π -meson in the decay of a V_1^0 -particle. The alternative possibility of a neutron two-prong star cannot, of course, be excluded.

The author would like to express his gratitude to Professor C. F. Powell for facilitating the exposure of the plates at high altitude as well as for providing laboratory facilities for their processing. He is also indebted to Dr W. O. Lock for helpful discussions. The event discussed was observed by Miss P. Ciok, to whom the author is obliged for her help, both in the measuring of grain-density and multiple scattering, and also in the preparation of the mosaic and the photo-micrograph.

Institute of Experimental Physics, University of Warsaw

REFERENCES

- [1] Danyasz M., Lock W. O. and Yecutieli G., 1951, Bristol Conference
- [2] Daniel R., Davies J. H., Mulvey J. M. and Perkins D. H., 1951, Bristol Conference.

Photo-Conductive and Photo-Voltaic Thallous Sulphide Layers

by

A. WOLSKA

Communicated by S. PIENKOWSKI at the meeting of February 23, 1953

I. Introduction. Since 1920, the year in which Case published his findings concerning thallous sulphide, the latter has been recognized as a photo-sensitive substance. In the years that followed, thallous sulphide was a subject of research for many investigators. The latest publications dealing with this substance appeared in 1944 [2], 1946 [3], [4] and 1947 [5]. Methods have been developed for the manufacture of so-called thallophe photo-cells which are sensitive to infra-red radiation.

The processes taking place in these photo-conductive layers have also been investigated. Until now, however, barrier effects [4], which play an essential role in micro-crystalline photo-sensitive films have not been taken into account when interpreting these processes.

New hypotheses, based on the theory expounded by L. Sosnowski in the publication: "Badania nad zjawiskami fotoelektrycznymi w półprzewodnikach" [6] and on the expected analogy with the known properties of PbS layers, have been adopted as the basis of this work. According to Sosnowski's theory, the photo-electric properties of a micro-crystalline layer are chiefly due to the presence of n-p contacts, i. e. potential barriers between the region of excess electro-positive centres (metal) and the region of excess electro-negative centres (oxygen).

Such a barrier is characterized by the following properties:

1. high dark resistance of a contact,
2. high photo-conductive sensitivity,
3. the appearance of photo-voltaic effect,
4. rectifying properties.

The aim of production is to secure a film with a mosaic structure of the n-p type. Such a film assumes some of the characteristic properties of a barrier, namely high resistance and a high degree of photo-sensitivity. The rectifying and photo-voltaic properties, however, are masked by chaotic

distribution of the barriers in the layer. By suitable activating treatment, resulting in the production of macro-regions of the "p" and "n" type in contact with each other, these properties can be given to the layer as a whole.

II. Analysis of the production method and its associated processes. In the method worked out by us, $\text{Tl}_2\text{S}_2\text{O}_3$ is the substance with which production is started. A quantity of this was supplied by the Department of Inorganic Chemistry, University of Warsaw.

A few milligrams of $\text{Tl}_2\text{S}_2\text{O}_3$ introduced into a production cell made of hard glass is then heated in a high vacuum at $450-480^\circ\text{C}$. This causes the substance to dissociate. It is undesirable to heat the substance to a higher temperature as this will result in the production of a non-conductive and not easily dissociative material of a yellow colour, consisting of oxygen sulphur and thallium.

A photo-sensitive layer, about 1 micron thick, is formed from the volatile products of the dissociation by evaporation onto the cooled wall of the photo-cell, which is provided with aquadag electrodes. These are in contact with tungsten electrodes which are fused into the side walls of the cell. Photo-sensitivity is achieved by oxygen treatment of the substance, both during the evaporation process and also after the formation of the layer. This treatment, lasting 2-3 minutes, is carried out in oxygen at low pressure (0.05-0.25 mm Hg), at a temperature of $250-300^\circ\text{C}$.

Oxygen introduced into the crystal lattice creates electro-negative impurity centers. Owing to the rapidity of all the processes the film has a non-homogeneous structure, excess and defective micro-crystals being mixed in it. We performed photo-voltaic activation by passing a constant current through the layer which is first heated to a temperature of $150-200^\circ\text{C}$, and then rapidly cooled. During this operation the oxygen ions move towards the anode and are "frozen" there. The layer acquires "permanent" photo-voltaic properties by the activation process which may be carried out equally well in vacuo as in oxygen.

Consequently, the first sensitizing process in oxygen during which, as a rule, changes in conductivity are observed, is at the same time an activating process. However, the next activation in vacuo increases photo-sensitivity. The best results are obtained by two activations in vacuo.

It should be noted that the passage of a direct current through the layer at room temperature, also gives it some photo-voltaic sensitivity. The effect, however, is not "permanent" and gradually disappears within a few hours or an even shorter period of time, whereas the slow disappearance of the "permanent" effect occurs over a period of years. The activation phenomenon at room temperature suggests that the barrier effect is due not only to the donor and acceptor impurity centers imbedded in the layer but also to surface phenomena.

In order to analyze the processes that take place during activation, the thermoelectric effect and the changes in conductivity and photo-con-

ductivity were investigated at various stages of production. A layer obtained by evaporation in vacuo of an initial product of dissociation obtained at 480°C , shows a negative thermoelectric effect and thus belongs to the "n" (electron) type. Such a layer is characterized by high specific dark resistivity and a low photo-sensitivity.

If such a layer is subjected to the sensitisation treatment in oxygen, the sign of the thermal E. M. F. is changed from negative to positive, and the conductivity is changed from the "n" to the "p" type (hole). This change is due to the appearance of oxygen centers in the crystal lattice. It is responsible too, not only for a considerable decrease in the resistivity of the layer but also for a substantial increase in its sensitivity. Too strong oxidation results in a decrease of sensitivity. A delay effect of the order of several minutes also appears. The return of such a layer to the "n" type of conductivity can be effected by subjecting the material to sublimation in vacuo at a temperature of $450\text{--}480^{\circ}\text{C}$. Such treatment reduces the amount of oxygen. It is accompanied by a substantial reduction and, in some cases even, the complete destruction of photo-sensitivity. The variations observed in thermo-electric power range from $+300\text{ }\mu\text{V/deg C}$ to $-100\text{ }\mu\text{V/deg C}$.

III. Methods of investigation. a) The spectral distribution of reactivity was investigated with the help of an infra-red monochromator equipped with a quartz prism. The radiation source was a tungsten incandescent lamp. Modulation of the illumination was effected by means of a revolving disc provided with rectangular openings, conforming to 700 light-impulses per second. The impulses of the voltage drop produced by a photo-current passing across a resistor connected in series with the cell and battery (or impulses of the voltage across the cell in the case of photo-voltaic effect) were applied between the grid and the cathode of the first valve of a selective amplifier (180000 voltage amplification). The absolute values of the reactivity in millivolts per microwatt per square cm of the incident radiation energy, were computed by comparing them with the known reactivity of PbS cells, calibrated with the help of a black body at 200°C .

b) The thermoelectric power was investigated by means of a bridge equipped with electrometric triodes. Owing to the very high resistance of the layers, it was impossible to use an ordinary galvanometer for this purpose. A difference in temperature between the two electrodes was effected by cooling one of them with a stream of compressed air, passed through a U-shaped pipe, immersed in a suitable thermostat. The temperature of the other electrode was maintained at a constant level by means of a stream of compressed air at room temperature.

c) The dependence of global sensitivity on temperature was investigated by means of a galvanometer. The layer was cooled by the evaporation of liquid air in which a heating spiral was immersed. The source of light was an electric 40 watt lamp provided with a lens.

IV. The properties of photo-sensitive layers. Sensitized layers possess the following characteristics:

1. A high specific dark resistivity contained within 10^2 — $10^7 \Omega \text{ cm}$ limits.
2. A sensitivity to radiation of a wave-length ranging between 0.4—1.3 microns.
3. A high value of photo-conductive reactivity, amounting in the case of average cells to as much as $200 \text{ mV}/\mu\text{W}/\text{cm}^2$ in the region of maximum sensitivity (0.83 microns).
4. A high value of photo-voltaic reactivity, amounting in the case of average cells, to as much as $3 \text{ mV}/\mu\text{W}/\text{cm}^2$ in the region of maximum sensitivity.

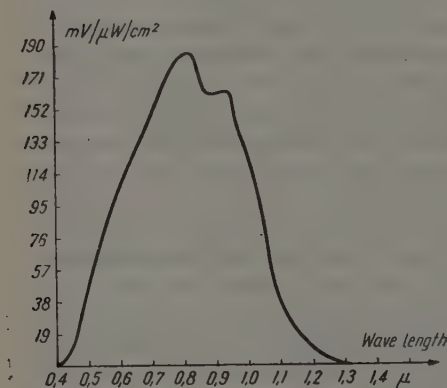


Fig. 1

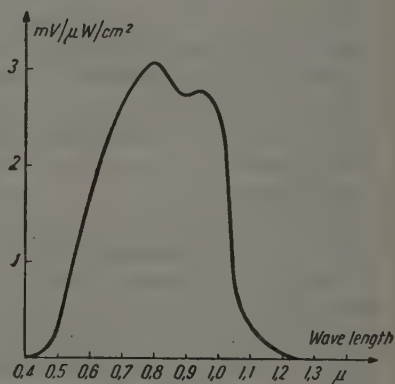


Fig. 2

5. An almost identical spectral distribution of the reactivity of both photo-conductive and photo-voltaic effects, as illustrated by the curves in Figs. 1 and 2.

6. Rectifying properties accompanied by a photo-voltaic effect.

7. An increase in the sensitivity with a fall in temperature, illustrated by the curve in Fig. 3.

8. An increase of the photo E.M.F. with a fall in temperature.

9. A relaxation time of photo-conductivity of the order of magnitude of a few milliseconds at room temperature.

This last phenomenon was investigated by L. Sosnowski and J. Ostrowski and forms the subject of a separate work.

The spectral distribution of the reactivity of both photo-electric effects was investigated jointly with L. Bobrowski. Spectral distribution of reactivity can be considered as characteristic for this type of layer, as it differs only slightly in each individual cell. This testifies to a common mechanism for the excitation of photo-sensitivity in all layers. The identity of the

spectral distribution of both effects suggests that the mechanism of excitation is common to both of them. The spectral distribution of reactivity agrees in general with that obtained for thallium sulphide by other authors [5], [7]. There are, however, some differences: instead of one flat maximum, as noted in the works cited, two maxima of reactivity were found by the author.

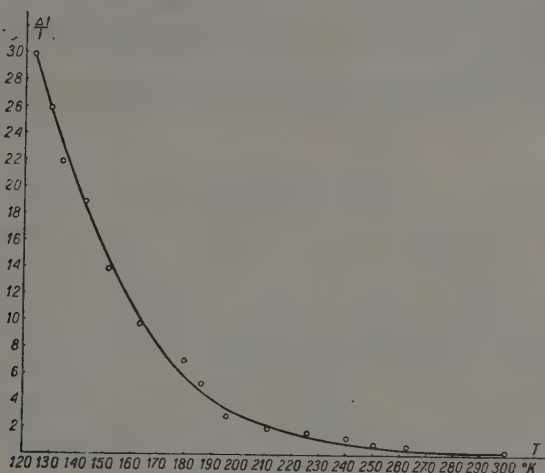


Fig. 3

The value of the reactivity of both photo-electric effects, as well as the specific resistivity of the photo-sensitive layers ought to be classified as structurally sensitive parameters which are not invariably characteristic of the substance. For example, a photo-conductive reactivity in the case of the most sensitive layers reaches a value 10 to 15 times greater than the average here indicated, while for the least sensitive it is 10 to 15 times smaller. The properties discussed here also show some variations in time. The resistance and sensitivity of activated layers enclosed in a high vacuum, generally increase during the first few days. This increase may be as great as 2 or 3 times the initial values. The photo-voltaic effect decreases slightly in the course of years. This fact can be ascribed to a slow diffusion of the oxygen impurity centers at room temperature. The photo-voltaic effect could very probably be preserved without change for a longer period, if the layer were kept at low temperature.

Grateful acknowledgments are made to Prof. S. Pieńkowski for allowing the author to work in the Physics Department of the University of Warsaw and to Prof. L. Sosnowski for suggesting the theme of the work, for his continued interest and his many valuable suggestions.

REFERENCES

- [1] Case T. W., Phys. Rev., **15** (1920), 289.
- [2] Starkiewicz J. Br., Pat. (1944), 3571/44, 3572/44.
- [3] Cashman R. J., Opt. Soc. Amer. **36** (1946), 336.
- [4] Hippel A., Chesley F. G., Denmark H. S., Ulin P. B., Rittner E. S., J. Chem. Phys. **14**—**6** (1946), 355.
- [5] Hewlett C. W., 1947, Gen. Electr. Rev. **50** (1947, April 22).
- [6] Sosnowski L., *Badania nad zjawiskami fotoelektrycznymi w półprzewodnikach*, Warszawa, 1949.
- [7] Reports on Progress in Physics, **11** (1946—47), 144.

Photo-Sensitive Lead Sulphide Layers with New Properties

by

T. PIWKOWSKI

Communicated by S. PIENKOWSKI at the meeting of February 23, 1953

The lead sulphide photo-conductive and photo-voltaic layers produced by the "evaporation" method [1] lose their photo-electric properties if contacted with atmospheric air and have to be enclosed in vacuum-tight, hard glass cells. It should be noted that the sensitivity of these layers deteriorates in the presence of oxygen already at a pressure as low as 10^{-3} mm Hg.

A method has been developed for the manufacture of sensitive layers, which are not impaired by air. Such layers maintain their photo-conductive and internal photo-voltaic properties in atmospheric air. A photo-voltaic effect arising from contact between the photo-conductive "open" layer and a metal electrode (Pb, Sn, Cu, Hg) has also been observed.

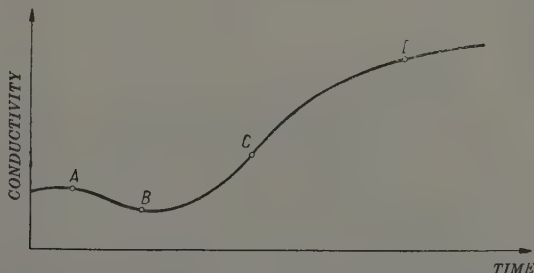


Fig. 1. Variations of conductivity with time during the sensitisation treatment

The initial processes intended to make a layer attain the state in which it is ready for sensitisation treatment are identical for both "open" and "vacuum" layers.

A small percentage of the layers show at this stage a small photo-conductive and photo-voltaic sensitivity which may be increased by the introduction of atmospheric air into the cell.

The proper sensitisation treatment, which concerns the totally insensitive layers, is controlled by observing the variations in conductivity with time (Fig. 1).

In order to obtain a "vacuum" layer, the latter has to be heated at 450 degrees C in oxygen at low pressure and the process suddenly stopped by rapid cooling at the moment when after an initial increase in conductivity of the layer (point *A*) followed by a decrease (point *B*), it again begins to increase (point *C*). A greatly prolonged heat treatment in oxygen, terminated by a rapid cooling of the layer (point *D*) is, however, required to sensitise an "open" layer. It is desirable to repeat this process several times. It has been observed that a layer so prepared shows photo-sensitivity both in vacuo and in air. The final process for increasing its sensitivity consists in heating the layer in vacuo, at 250 degrees C, while simultaneously passing a current through it for a time long enough to destroy its sensitivity. As soon as this has been done and the temperature of the layer has dropped to below 250 degrees C, air is introduced into the cell and the layer is cooled rapidly to room temperature.

The photo-electric properties of the oldest cells processed in this manner two years ago have not deteriorated to date.

The lowest detectable intensity of radiation, the spectral responsivity (Fig. 2), and the response time (20 - 180 microseconds)* of photo-conductive

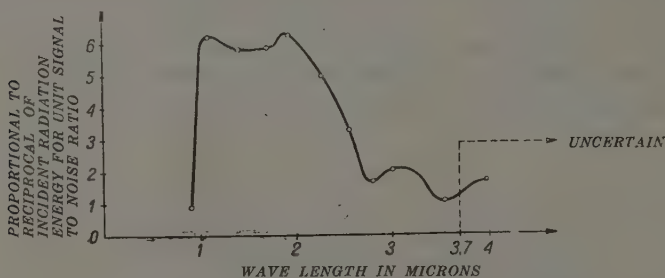


Fig. 2. Spectral response of a lead sulphide "open" cell. Radiation interrupted 800 C/sec

"open" cells do not differ essentially from those of the vacuum-tight layers. The accessibility of an "open" layer gives the latter an obvious advantage over one that is enclosed, as it furnishes additional possibilities for experimentation.

It is worth mentioning that the dark resistance and the photo-conductive sensitivity of an open layer immersed in a liquid air bath are many times (over a hundred-fold) greater than those of a layer exposed to air at room temperature.

*) The response time was measured by M. Chmielewski and J. Ostrowski.

The assumption that specks of lead (microcrystals) are formed throughout the layer may serve to explain the photo-electric effects observed and also specifically their insensitiveness to atmospheric air. Their appearance may be ascribed to the contacts such specks make with the semi-conductive microcrystals of the layer. Such a hypothesis seems to be acceptable in view of the photo-voltaic contact effect observed.

A metal semiconductor contact photo-voltaic effect can perhaps be partly explained in terms of the excess-defect semi-conductor model advanced by L. Sosnowski [2] on the basis of the known experimental fact concerning the mutual diffusion of atoms and/or ions (impurity centers) when one solid is in contact with another.

Analogy with phenomena appearing in photo-sensitive layers prepared from other substances suggests that similar photo-sensitive "open" layers may possibly also be made of them.

The author is grateful to Professor S. Pieńkowski for enabling him to carry out this study and to Professor L. Sosnowski for valuable discussions and for his interest and encouragement shown during this research work.

Institute of Experimental Physics, University of Warsaw

REFERENCES

- [1] Sosnowski L., Starkiewicz J. and Simpson O., *Nature* **159** (1947), 818.
- [2] Sosnowski L., *Phys. Rev.*, **72** (1947), 641.

The X-ray Investigation of a Group of Fossil Rubbers

by

J. AULEYTNER

Communicated by S. PIENKOWSKI at the meeting of January 12, 1953

The present work aims at the structural analysis of certain fossil rubbers dating as far back as the Eocene, Miocene and Pliocene periods. The investigations which were made were concerned with physico-chemical problems on the one hand, and paleobotanical and geological on the other.

Samples of rubber were kindly lent to us by the Botany Department of the Jagiellonian University, Cracow. These samples were from Professor Szafer's collection. All data relating to the nomenclature, age, derivation, as well as the conditions under which these specimens were found, are given in Table I.

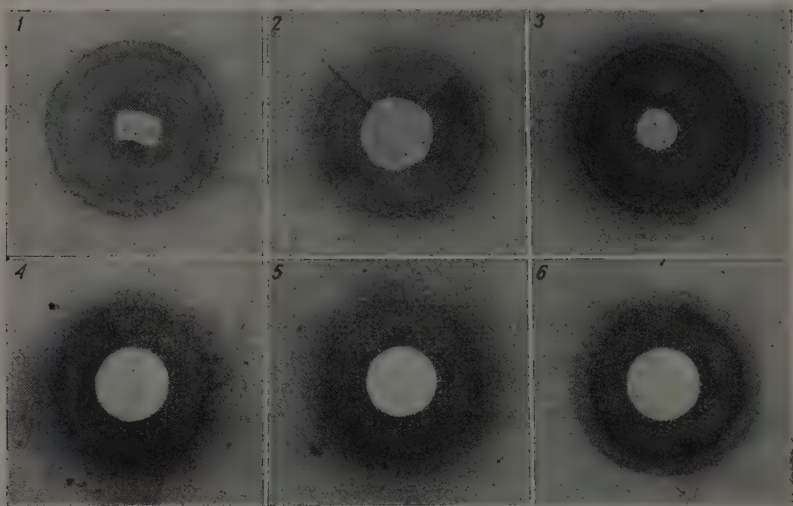
TABLE I

Contemporary Rubbers: Delachampia, Manihot Glaziovii, Ficus Elast., Castilloae — a uniform hardened mass, elasticity poor, museum samples, age 40 yrs.
Fossil Rubber from Leopolds Grube, (German Democratic Republic): fibres 0.15 mm in diam., elasticity very good, discovered by Prof. Gothan, 1947-1950 in layers of brown coal, Eocene, age approx. 30 mil. yrs.
Eucommia Ulmoides — contemporary, a bundle of fibres, 4×10^{-4} cm in diam., elasticity poor, from seed.
Eucommia Europea — Higher Pliocene, 600 thous. yrs., elasticity good, a bundle of fibres a/m.
Eucommia Ulmoides — Stare Gliwice, Miocene, approx. 10 mil. yrs., from seed of fibres discovered in loam, fibres a/m.

Polanyi's method was used for investigating the samples. The patterns formed by the interference of X-rays diffracted on the lattices of the substances examined were registered on photographic flat films. The interference patterns were then photographed under exactly the same carefully maintained experimental conditions. Thus it was possible to compare the patterns of the various samples. To check whether the impurities present had any effect

on the interference patterns, some specimens were dissolved in chloroform, and the interferences characteristic of each substance which had been precipitated by ethyl alcohol and extracted, were then photographed. X-ray patterns were also produced by a non-solvent component. The positions of the interferences in the heat-treated specimens under examination were also investigated. The effects of slightly stretching both contemporary and Eocene rubber were also studied. In order to ascertain the degree of diffusion of the rings and the measurements of their relative blackening the diameters of the rings were examined with a microphotometer. With this apparatus the interference patterns were obtained in the form of Debye-Scherrer rings from the diminutive rubber samples of 0.25 mm in diameter.

The exact analysis of these rings has made possible assignment of certain details in the crystalline structure of the substances examined and permitted the determination of the characteristic lattice constants. For purposes of comparison, samples of different but related contemporary natural rubbers were also investigated by means of X-ray analysis.



Photos. 1 - 6

The Result of X-ray Analysis. The existence of two types of interference rings corresponding to the structure of the samples were determined. The patterns of one type appeared to be identical with those characteristic for contemporary rubber (Photos. 1, 2), and the patterns of the other type with those for gutta-percha (Photos. 4, 5, 6). No. 1 patterns were obtained with contemporary rubber (family — Euphorbiaceae, type — *Dalechampia-Bidentata*) from Java. The interference patterns consist of five

distinct rings. Their features, briefly enumerated, are as follows: i) A relatively large diffusion of the 2nd and 3rd rings (from the centre) is seen as well as a strong blackening of the background in the region of the radius of the 3rd ring. ii). No Laue interference spots are to be found on any of the rings. iii) An increased blackening of the background round the lead diaphragm may be noticed. The data regarding the periods determined and the ratios between the blackenings are given in Table II (first row).

The interference patterns obtained in the case of both fossil rubbers (left and right photographs 2) dated from the Eocene Period and contemporary (top-bottom) are compared and shown alongside in Photos. 2.

The numerical data are given in Table II.

TABLE II
Comparison of Periods

Name	1 ring $d(\text{\AA})$ s_1	2 ring $d(\text{\AA})$ s_2	3 ring $d(\text{\AA})$ s_3 $s_2:s_3$	4 ring $d(\text{\AA})$ s_4 $s_3:s_4$	5 ring $d(\text{\AA})$
Contemp. rubb.	6.43 93.6	5.03 95.0	4.34, 90.8, 1.046	3.78, 72.8, 1.302	3.40
Rubb. from Eoc.	6.43 87.4	5.02 90.8	4.34, 85.1, 1.066	3.78, 69.3, 1.296	3.40
Eucom. Ulm. Cont.	4.83 84.9	3.86 68	3.36, 31.6		
Eucom. Europ. from Pliocene	4.71 90.7	3.86 84	3.33, 74.8	2.82	2.58
Eucom. Ulm. from Miocene	4.83 89.1	3.86 84	3.36, 72.6	2.82	2.58

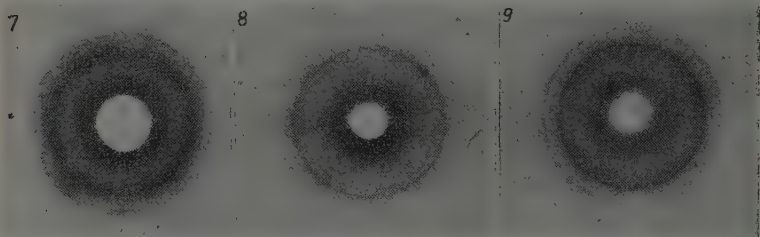
In column s_1 — are given the percentages expressing the various ratios of the blackening on the ring to the complete blackening on the photographic plate.

In column d — are given the periods corresponding to each ring.

The interferences obtained in the case of slightly stretched contemporary rubber are shown in Photo. 3. Polanyi's arcs which are characteristic of substances possessing a distinct paratropic orientation, are seen on the first ring from the centre. Slightly stretched rubber belonging to the Eocene period was also subjected to irradiation by an X-ray beam falling at right angles to the long axis of the fibre, but nothing similar to the above-mentioned arcs was observed. The results (see Table II) of the investigations with regard to contemporary rubbers for which the X-ray method was employed, show that the latter have an identical crystalline structure and are characterised by identical interplanar spacings. Both the fossil and contemporary rubbers, when heated to a temperature of about $+36^\circ\text{C}$, are characterized by a largely diffused ring, proper to an amorphous substance with an interplanar spacing of 4.9 \AA .

The specimens of contemporary "rubber" and of rubber from pits, dating from the Miocene and Pliocene periods, are characterized by rings of the

second type (Photos. 4, 5, 6). In all three photographs two rings may easily be recognized with the first ring from the centre largely diffused. The X-ray patterns for the sample of *Eucommia* U. from the pits consist of three rings with numerous Laue interference spots. The positions of the next two rings may accordingly be determined by some Laue spots. The photograph of *Eucommia* *Europae* interferences consists of Laue spots equally distributed on the 3rd, 4th and 5th rings from the centre. Interference patterns No. 6 were obtained for *Eucommia* U. (contemporary). Only two rings are seen. In all three photographs a strong blackening of the background round the lead diaphragm may be noticed. A characteristic blackening in the background of the radius region of the 2nd ring is also easily seen. *Eucommia* U. (contemporary), when heated to a temperature of 36° C and then cooled to room temperature, gave patterns of the type No. 7. The appearance of a third distinct ring can be observed. In the background of the first diffused ring a sharp maximum along the whole circle has also appeared. The sample of *Eucommia* U. from the pits, with the large crystallites mechanically removed, heated to a temperature of approx. 36° C, and then cooled, gave interferences of the type No. 8. Many Laue interference spots are present on the 5th ring. To make comparison possible, photograph No. 9 is given. It shows the interference patterns for samples of *Eucommia* *Ulmoides* (contemporary) which had been dissolved in chloroform, precipitated from the solution and then dried.



Photos. 7—9

In connection with the strong blackening of the background in the central part of the interference patterns, the X-ray scattering from the collimator edges and lead diaphragm was investigated, and found to be due partly to the small-angle scattering of X-rays.

Conclusions.

1. From the analysis of the patterns obtained, and by determining the number of lattice constants, it can be shown that one system of interference rings is characteristic for rubber and another for gutta-percha.

2. Eocene rubber (approx. 30 mil. yrs.) is identical in structure with contemporary. These two rubbers, however, differ from one another to

a great extent as regards such physical properties as elasticity and material strength. The fossil rubber has very good elasticity, in spite of its crystalline structure.

3. The specimens derived from the *Eucommia* samples are simply gutta-percha. They have a crystalline structure. The pit samples contain also larger crystallites of two different types as regards their lattice constants. In the fossil samples from Miocene, one form of these crystallites predominates over the other (Photograph 4 with many interference spots on the 3rd ring).

4. It is worth noting that despite the long period during which it underwent the enormous pressure of coal layers, and despite its fibrous structure, the fossil rubber does not show an order of arrangement with any orientation of the crystallites.

5. When the elasticity of fossil rubber is considered it appears that its properties are due to complexes of the molecules rather than to the interior structure of the crystallites.

6. It may be supposed that the ageing process of rubber can be stopped in certain circumstances and the balance in this case is very stable.

7. The fact that a small-angle scattering was obtained in the substances examined proves the existence of regions of linear size varying from 10\AA to several hundreds \AA , these being differentiated in accordance with their electron density.

The author is much indebted to Professor S. Pieńkowski for suggesting the problem and for his helpful discussions and valuable criticism throughout the course of the work.

Institute of Experimental Physics, University of Warsaw

Phosphate Coatings on Zinc and its Alloys

I. Phosphate Treatment of Zinc in $\text{Mn}(\text{H}_2\text{PO}_4)_2$ Solutions

by

J. KAMECKI and T. DRWAL

Communicated by B. KAMIENSKI at the meeting of January 19, 1953

Since the year 1929 phosphate coatings have been increasingly used in the protection of zinc and its alloys from corrosion. Previous to this, solutions suitable for the phosphatizing of iron and steel were used for this purpose. Later, however, it was found that better results could be obtained if special solutions were used. Many papers have been published on this subject [1], [2] but the majority of them were patents or reviews and so there are still many problems which have not yet been elucidated and the present technical solutions cannot be considered as being ideal [3], [4].

The aim of the present research was to find the composition of a phosphate-bath that would give the best technical results and also to examine the properties of the coatings obtained. A phosphate bath usually contains primary iron (II)-zinc- or manganese phosphate solution with some free phosphoric acid excess. A very good quality of phosphate coatings obtained by Wulfson and Simiakowski [5] on zinc in a "Masheff" solution induced us to undertake investigations with regard to primary manganese phosphate solutions. From the conditions of equilibria in system $\text{MnO}-\text{P}_2\text{O}_5-\text{H}_2\text{O}$ given in some previous papers we attempted to calculate the composition of the best phosphatizing solution. Our attempts having proved unsuccessful we decided to find this composition by empiric means.

EXPERIMENTAL PART

1. Composition of solutions, apparatus and technique. Using chemically pure reagents, nine different phosphatizing solutions were prepared. Their composition is given in table I.

A beaker containing a phosphatizing solution was placed in an oil-filled thermostat. The temperature of the thermostat was kept automatically at $98^\circ \pm 0.5^\circ \text{C}$. The experiments were carried out with zinc NO (PN-H-82200)

TABLE I
The composition of phosphatizing solutions

Symbol of the solution	The composition of the bath				The ratio of free H_3PO_4 to combined H_3PO_4
	$Mn(H_2PO_4)_2$		free H_3PO_4		
	mol/l	g/l	mol/l	g/l	
I	0.1	24.89	0.01	0.98	1: 20
II	0.1	24.89	0.02	1.96	1: 10
III	0.1	24.89	0.03	2.94	1: 6.67
IV	0.1	24.89	0.04	3.92	1: 5
V	0.1	24.89	0.08	7.84	1: 2.5
VI	0.2	49.78	0.06	5.88	1: 6.67
VII	0.4	99.56	0.12	11.76	1: 6.67
VIII	0.8	199.12	0.24	23.52	1: 6.67
IX	0.2	49.78	0.04	3.92	1: 10

and zinc alloys ZNAL 40, 41 and 43(PN-H-87101). The specimens were cut off from a bar, planed by means of a shaping machine and polished with emery papers up to number 4/0. The time required for the phosphate treatment could not be assumed from any previous work, because different data are given. Therefore in each phosphatizing solution the relation between immersion time and the quality of the resultant coating was investigated. Six identical plates of NO zinc were phosphatized for periods of 10, 20, 30, 40, 50 and 60 minutes and the quality of the coatings produced was examined by means of the drop test.

2. Drop test. The drop test is a special, simple, rapid method for examining the resistance to corrosion of protective coatings. The practical application of this method for the examination of phosphate coatings on iron and steel was made possible thanks to the work of G. Akimov and A. Ulyanov. We tried using their reagent to examine phosphate coatings on zinc but the results were not good. After many experiments it was established that the following composition constituted a suitable reagent for the examination of phosphate coatings on zinc: NaCl 3g, HCl 0.01 N 10 ml, $CuSO_4 \cdot 5H_2O$ 8g distilled water to 100 ml. The end of the drop test was accepted as coinciding with that moment when the surface beneath the corrosive solution was completely covered with a black or red copper deposit. The time taken by the drop test was measured by means of a stopwatch. The forming of a copper deposit was observed with the naked eye. For untreated zinc and ZNAL alloys the time required for the drop test when using the solution described above was not more than three seconds. Phosphate coatings of poor protective value had a drop test resistance of between 20 seconds and 2 minutes, better coatings from 2 minutes up to ca. 60 minutes.

3. Results. The first series of solutions had the same primary manganese phosphate content and increasing free phosphoric acid content (solutions I, II, III, IV and V). The various phosphatizing times were 10, 20, 30, 40, 50 and 60 minutes. The quality of the coatings obtained on NO zinc was examined by means of the drop test. The results are given in table II.

TABLE II

Results of the drop test examination of phosphate coatings produced on NO zinc in solutions with increasing free phosphoric acid content

Phosphatizing time in minutes	The time of the drop test in minutes on coatings produced in solution				
	I	II	III	IV	V
10	1	5	5.9	0.3	0.17
20	3.8	9.3	12	0.9	0.8
30	6.5	10	15	1.25	1.1
40	9.5	13	22	2.25	1.3
50	11.5	15	30	3.8	2.4
60	7.75	9.7	18	3.1	1.9

It is evident that the best coatings are produced in solution number III in which the ratio of free phosphoric acid to combined phosphoric acid is 1:6.67.

Consequently the quality of the phosphate coatings produced on NO zinc in solutions with increasing primary manganese phosphate concentration and constant free phosphoric acid to combined phosphoric acid ratio (1:6.67) was investigated. The results of the drop test examination are recorded in table III.

TABLE III

Relation between the concentration of the phosphatizing solution, the time of phosphate treatment and the quality of phosphate coatings produced on NO zinc

The time of the phosphate treatment in minutes	The time of the drop test in minutes on coatings produced in solution				
	III	VI	VII	VIII	IX
10	5.9	30	45	58	23
20	12	37	70	96	27.5
30	15	57	75	67	44
40	22	52	60	57	38.7
50	30	49	53	46	33.5
60	18	45	50	32	29

In the solutions with higher primary manganese phosphate content (the ratio of free to combined H_3PO_4 being constant) the quality of the coatings produced is higher and the time required for the formation of the best coating is shorter. A good phosphatizing solution, however, must give coatings of uniform quality that will last over a long period of time. In the phosphatizing process the efficiency of the solution depends not only on the quality of the coating obtained but also on the speed at which the so-called aging of the bath takes place (i. e. its progressive loss of efficiency). Therefore a further series of experiments were made in order to examine the progressive loss of efficiency (the aging) of solutions III, VI, VII and VIII as a function of the area of the metal surface phosphatized previously. The results of these experiments are recorded in table IV.

TABLE IV

The quality of phosphate coatings produced on NO zinc as a function of the area of the surface previously phosphatized (the aging of the bath)

Sample number	The area of the surface phosphatized previously $cm^2/liter$	The time of the drop test in minutes on coating produced in solution			
		III	VI	VII	VIII
1	0	10	34	57	80
2	250	10.75	33.5	56.5	78
3	500	10.25	32.5	54	71
4	750	10.1	31	48	56
5	1000	9.75	30	40.75	13
6	1250	9.0	27.5	20	3.6
7	1500	7.5	25	12	1.75
8	1750	7.4	21	4.5	1.25
9	2000	7.25	18	2.8	—
10	2250	7.0	15	1.2	—
11	2500	6.7	8	1.0	—
12	2750	6.6	6.5	—	—
13	3000	5.9	5.3	—	—
14	3250	5.6	3.2	—	—
15	3500	5.3	2.7	—	—
16	3750	5.25	1.5	—	—
17	4000	4.75	1.2	—	—
18	4250	3.1	1.0	—	—
19	4500	2.5	0.9	—	—
20	4750	1.25	—	—	—

As a result of three series of experiments, solution number VI was considered on the whole to be the best (high coating quality and relatively

slow aging). The best phosphate coating obtained in this solution was then examined by means of a quantitative corrosion test in 3% NaCl and 0.1 % H_2O_2 solution. The results of this test confirmed the justness of the conclusions arrived at on the basis of the drop test. Zinc alloys ZNAL 40, 41 and 43 were phosphatized in solution VI which gave the best results on NO zinc. The drop test showed that the coatings thus produced had less protective value than those produced on zinc.

DISCUSSION AND CONCLUSIONS

The drop test devised for phosphate coatings on zinc and its alloys proved successful in practice.

The results of our investigations show that by a simple empirical method (only nine solutions were investigated) it is possible to establish which kind of composition gives the best solution for phosphatizing NO zinc. The best results were obtained in solution number VI, at a temperature of 98°C; the duration of the phosphatizing treatment was 30 minutes. All the curves representing the quality of the phosphate coatings produced in the solutions used in our research show a characteristic maximum which is dependent on the phosphatizing time. This maximum of the quality of the coatings is undoubtedly the result of the twofold action of the phosphatizing time: the coating becomes thicker but at the same time the phosphate crystals grow and their increase in size lowers the quality of the coating. The growth of the crystals was confirmed by microphotographs of the coatings produced during the different periods of immersion.

The unfavourable results of the phosphate treatment of zinc alloys ZNAL are due to the latter's Al content [2]. Therefore the composition of the phosphatizing solution for these alloys must be worked out separately.

Academy of Mines and Metallurgy, Department of Physical Chemistry and Electrochemistry, Cracow

REFERENCES

- [1] Krause R., *Korr. u. Metallschutz*, **20** (1944), 167.
- [2] Machu W., *Die Phosphatierung, Wissenschaftliche Grundlagen und Technik*, Berlin, 1950.
- [3] Macchia O., *La protection phosphatique des metaux ferreux*, Paris, 1944.
- [4] Halls E., *Metalurgia* **37** (1948), 299.
- [5] Simiakowski A. and Wulfson W., *Doklady Ak. Nauk S.S.S.R.* **46** (1945), 251.
- [6] Akimov G. and Ulyanov A., *Uskoriennyye metody zaschity izdieli ot korozii*, Moskwa, 1946.

Coal Tar as a Typical Polyazeotropic Mixture I

by

W. ŚWIĘTOSŁAWSKI

Communicated at the meeting of January 12, 1953

1. Polyazeotropic Systems. Three kinds of polyazeotropic systems have been examined. In previous papers [1] we use the term "positive polyazeotrope" for designating a system in which agents A , B and C , both separately and in combinations of two or three, can form with a series (H) of homologues, their isomers or other closely related substances, positive azeotropes of the general types (A, H_i) , (A, B, H_i) and (A, B, C, H_i) .

If a weak acid (A) forms with a homologous series of weak bases (P) a number of negative azeotropes $[(^-)A, P_i]$, or if a weak base (P) forms with a series of weak acids (A) a similar series of negative azeotropes $[(^-)P, A_i]$, we call them negative polyazeotropic systems [2].

Finally, any negative azeotrope $[(^-)A, P]$ may form with a series of homologues and their isomers (H) a positive-negative polyazeotropic system $[(^-)A, P (+)H_i]$ [3]. Quaternary positive-negative azeotropes of the general type $[(^-)A, P (+)B, H_i]$ are as yet unknown; their existence, however, is very probable [4].

2. Polyazeotropic Mixtures. Mixtures of two or more polyazeotropic systems will be referred to as polyazeotropic. According to this nomenclature, low and high temperature coal tar, petroleum, synthetic liquid fuels and similar liquids should be regarded as polyazeotropic mixtures. It should be emphasized that the number of components forming polyazeotropic mixtures and their concentrations may vary to a very large extent in different liquid mixtures. Of these numerous polyazeotropic mixtures, coal tar is the most complicated because of the number of homologous series, the constituents of which each play their part in the formation of different kinds of azeotropes.

3. Main Component of a Polyazeotropic Mixture. For a proper understanding of the complicated phenomena taking place in the course of a batch distillation of different oils separated from coal tar, it is important to find out whether or not in the oil being distilled there exists

a substance in sufficient quantity to form with other constituents all the azeotropes which might be formed under a certain pressure established in the distillation still. This substance will be called, both in this and in the other papers of this series, the main component of the polyazeotropic mixture.

In a middle oil, naphthalene is the main component, because it is present in such a quantity, that at the end of the distillation, besides the azeotrope formed by it, its excess appears as a "zeotropic component" in the fraction collected. At the final moment of the distillation, the distilling curve reaches the horizontal line corresponding to the boiling temperature of pure naphthalene: 218.2° C. Some time later fractions are collected at successively increasing temperatures. From then on almost tangent zeotropes [5] of naphthalene with higher boiling constituents of the mixture are collected in the receiver.

In Fig. 1 is shown a typical distilling curve obtained for a middle oil.

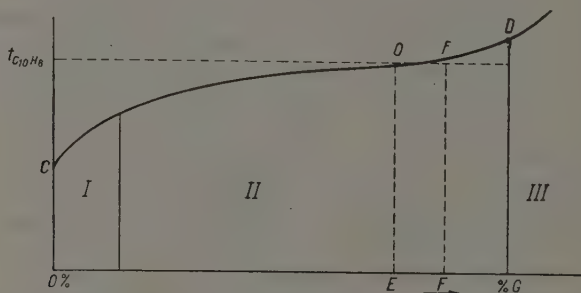


Fig. 1. Distilling curve obtained for a batch distillation of a middle oil. Part II corresponds to that fraction in which numerous azeotropes formed by naphthalene with other constituents are collected in the receiver

Similar shapes of distilling curves may be obtained for other polyazeotropic mixtures, in which the main component is present.

The horizontal line drawn through a point representing the boiling temperature of the main component is called the azeotropic ceiling line.

If a large excess of the main component is present, some fraction of the distilling curve merges with the azeotropic ceiling line. On the other hand, a large number of high boiling constituents of the mixture exerts their influence on the composition of the distillate. For this reason the distilling curve may cross the ceiling line at an acute angle. This case is shown in Fig. 1. Such a phenomenon occurs when a middle oil is submitted to a fractional batch distillation. Higher boiling isomeric methylnaphthalenes are responsible for the absence of that section of the distillation curve which merges with the azeotropic ceiling line.

4. Polycomponent Azeotropic Agent for Naphthalene Removal. The mother liquor, obtained after the naphthalene crystals have been removed by any one of the known procedures, represents a typical mixture of substances which, taken together, may be considered as a polycomponent azeotropic agent for the azeotropic removal of naphthalene from any oil containing this substance.

Extensive research and numerous experiments carried out by a group of Polish researchers on laboratory, pilot-plant and industrial distilling instalations have proved that the recycling of a polycomponent azeotropic agent favours its self-improvement. In fact, in each cycle the azeotropically inactive constituents are automatically removed from the main fraction in the course of distillation. They are found either in the forerunnings or in the higher boiling fraction and bottom product, respectively.

5. Final Remarks. The example in which naphthalene is the main component should be considered as a typical one for any polyazeotropic mixture. In other batch distillations similar phenomena can be observed in all those cases in which the main component is present. Some of these cases will be described in other papers of this series.

SUMMARY

1. Definitions of the terms: polyazeotropic system, polyazeotropic mixture, main component, azeotropic ceiling line and polycomponent azeotropic agent are given.

2. Low and high temperature coal tar, petroleum, synthetic fuels etc. are considered as polyazeotropic mixtures. It has been emphasized that coal tar is the most complicated polyazeotropic mixture yet examined.

3. The distillation of a middle oil has been used as a typical example of the way in which naphthalene forms numerous azeotropes with other tar constituents and plays the role of the main agent.

4. The mother liquor obtained after the removal of naphthalene crystals has been found the most suitable polycomponent agent for azeotropic removal of naphthalene from tar oils.

5. The recycling of the polycomponent azeotropic agent favours the removal of constituents which are unable to form azeotropes with the main component. In that way, in the course of recycling, a self-improvement of the azeotropic agent takes place.

6. The phenomena found when naphthalene is the main component resemble those which are typical of other polycomponent mixtures.

Department of Chemistry, University of Warsaw

REFERENCES

- [1] Świętosławski W., *On polyazeotropic Positive Systems*, Bull. Soc. Chim. Belg., 62 (1953), 10-20.
- [2] Świętosławski W., *Classification of Negative Azeotropes*, XIV, Bull. Acad. Polonaise, Sci. 1 (1953), 63.
- [3] Świętosławski W., *On Ternary Positive-Negative Azeotropes*, XV, Bull. Acad. Polonaise, Sci. 1 (1953), 66.
- [4] Świętosławski W., A paper not yet published.
- [5] Świętosławski W., Bull. Acad. Sci. Polonaise, 19-28 1950 A.

The Problem of »Kalification« of Magmatic Rocks in the Region of Cracow

by

J. TOKARSKI

Communicated at the meeting of February 23, 1953

In 1909, Z. Rozen published a study entitled »The old lavas of the principality of Cracow«, in which he dealt mostly with the microscopical and chemical physiography of porphyries, diabases and melaphyries of that region. He found a particularly high concentration of potassium oxide in some specimens of magmatic rocks which he examined and also in the accompanying tuffs, and he endeavoured to explain this fact by a special kind of secondary geochemical changes as yet unknown in the study of rocks. These changes, which Rozen called »kalification«, were, according to him, caused by particular physical and chemical conditions which arose during the final phase of consolidation of old Cracow lavas and their tuffs, just before their simple hydrolisation in the form of kaolin. According to Rozen, the rock constituents that underwent »kalification« were above all plagioclases, within the phenocrysts, as well as in the groundmass. During the process, the soda feldspar (albite) and calci feldspar (anorthite) which they contained, were transformed into particles of potash feldspar (orthoclase). Thus the quantity of potassium in porphyries was raised from 3.67% to 6.28%; in tuffs, which are closely connected with them, the increase was even more marked, namely up to 9.4% in the case of Filipowice tuffs.

The author of the study restricted himself to presenting these facts to the public without giving any sort of documentation to the hypothesis put forth by him, concerning the process of »kalification«. This documentation might undoubtedly have been presented, had he examined microscopically the structural transformation of minerals of a large number of microscopical slides of rock samples.

In 1939, A. Bolewski tried to clear up finally the process of »kalification«. On the basis of detailed chemical analyses of samples collected primarily in parts of the Miękinia quarries, he showed that this process never took place at all. According to this author, the magmatic rocks of

the district of Cracow, richer in potash than the Miękinia porphyries, form a special class, which is »a priori« richer in potash feldspar. They belong also to the trachyte type.

However, neither of the authors quoted above drew attention to the characteristic transformations that were accomplished within the minerals composing these Cracow rocks. These changes are perfectly discernible in microscopic pictures. Only Z. Rozen pointed out that »kalified« minerals were covered with spherulitic aggregates, visible only with crossed Nicols. They are not visible without polarizers, and the respective individual feldspars appear to be fresh, untouched crystals. Neither does the systematic incorporation of »kalified« rocks into the trachyte group clarify the question of transformation of feldspars into the spherulitic aggregates mentioned above.

We are of the opinion that an exact explanation of the phenomenon of transformation of feldspars is in this case of essential importance. During the last few years the author worked on the problem of a practical utilization of Filipowice tuffs, which are extremely rich in potassium, especially in the vicinity of Kowalska Góra. According to Z. Rozen they attained a high degree of »kalification«, so we gave careful attention to the microscopic physiography of the feldspars in their phenocrystic forms and in the groundmass. The results of our studies, which were carried out collectively, will be published in detail at a later date. Here, we have only assembled those facts which directly concern the »kalification« process itself. They are the following:

1. Filipowice tuffs have a special mineral and chemical composition. Their principal salic minerals are sanidines, which are developed either as phenocrysts or fine components of the groundmass. Their principal characteristic is an absolute lack of plagioclases. Sanidine belongs to the crystal type having a small optic angle, an optic plane parallel to M, and low refraction indices of less than 1.535 (Canada balsam). Birefringence is low, being about 0.005. The femic constituents are in most cases completely destroyed, with the exception, at times, of large, idiomorphically developed biotite plates. Their groundmass, seen through a microscope, clearly shows a number of thin sanidine fibres, which become visible only after their red, iron-coloured dye, dispersed in the form of a powder in the rock material, is removed by means of strong hydrochloric acid. Among foreign elements, the principal ones are fragments of trachyte rocks (containing no quartz), mainly composed of sanidine. Some of these bring vividly to mind the well-known sanidine trachytes of Drachenfels. One typical analysis of this tuff gave the following results:

SiO ₂	65.36%	CaO	0.3%	K ₂ O	9.68%
Al ₂ O ₃	17.28%	MgO	trace	Na ₂ O	1.99%
Fe ₂ O ₃	5.49%				

Planimetric analysis of the same sample showed a volumetric content of: (in per cent.)

quartz	10,
sanidine (with spherulites)	87,
biotite	2,
iron oxides	1.

A similar analysis of a sample of Drachenfels trachyte was shown to contain:

quartz	8%	biotite	5%
sanidine	65%	magnetite	3%
plagioclase (oligoclase)	19%	apatite	traces.

From these figures it follows clearly that Filipowice tuffs are closely related to orthosite or K-trachyte magma (according to Johansen's classification).

On the other hand, Miękinia porphyries originate from granodiorite magma and so should — as a product of lava flows — be called «rhyodacites».

These types of rock are not directly connected with one another, even though they were found to be contacting topographically. Thus the thesis, presented by A. Bolewski, concerning the appearance of trachytes in Cracow magmatic rocks, appears to be correct.

2. Precise investigations of a large number of thin microscopical sections of Filipowice tuffs, corresponding to samples collected in various parts of the country, proved that not even traces of plagioclase could be found in them. This was also confirmed by special research work, carried out on pulverized material in considerable quantities, whose average samples were enclosed in microscopical slides by Canada balsam. These investigations proved that — besides quartz and «spherulites» — all other components found here (mainly sanidine fragments) had a lower refraction index than balsam. Therefore, they could not be plagioclase, especially rich in anorthite, like that found in the feldspars among the Miękinia porphyritic phenocrysts.

The chemical analysis of Filipowice tuffs, referred to above, showed only 0.3% of CaO, hence there were only traces of anorthite present.

3. The spherulite aggregates we have mentioned, are the mysterious mineral which was said to be the product of the «kalifikation» process. Our work has proved that the principal mineral in tuffs and «kalified» porphyries is sanidine, which is developed both in the shape of phenocrysts and as part of the fine-grained groundmass. Sanidine phenocrysts are quite normally developed here and do not differ optically from the forms of that mineral known so far.

Primitive sanidine is completely or partly transformed into spherulites. In the latter case the spherulites collect in the central part and are also to

be found in the groundmass. Their structure is generally that of centripetal fibres, proceeding in rays from a central point, with a direction of optical elasticity gamma along their elongation. Due to the fairly regular disposition of these fibres, the rim of the spherulites has a uniform refraction index. Already the observation of Becke's line on the contact margin of the spherulites with either Canada balsam, sanidine or the available fragments of quartz, showed their higher index of refraction. The latter was precisely fixed by means of a mixture of oils serving as an immersion medium, and the figure of 1.58 was obtained for spherulites.

The light refraction index, established in the same manner, vertically to the elongation of the spherulitic fibres, was somewhat lower. One might infer from this that spherulitic aggregates are not highly birefringent, and this was confirmed by the observation of the interference colour, which was found to be lower than for the same thickness and orientation of quartz.

Unfortunately, in spite of studying thoroughly over 200 preparations of Filipowice tuffs, we did not find any other form of that mineral outside spherulites. It was, therefore, impossible to carry out any further precise optical, and above all conoscopic, determinations. Nevertheless, the high index of light refraction of spherulites clearly proved that they could not belong to potash feldspars and plagioclase minerals, which were optically determined, with the exception of bytownite, anorthite or celsian links. Hence their nature could only be established through a precise chemical analysis of the spherulites separated from the rock. Attempts at separation failed, in spite of considerable effort. It turned out, namely, that spherulites are very closely associated by their specific weight with sanidine. Therefore, as a rule, they passed to the lighter fraction, together with their major component, sanidine, when separated with the aid of bromoform. So we decided to submit to chemical analysis a mixture of both components, namely sanidine and spherulites. After numerous attempts, we obtained a sample which, under the microscope, proved to contain almost exclusively these two elements. Quantitative microscopic examinations of the powder showed a quartz content of only 2%.

The results of chemical analysis were the following:

SiO ₂	67.35% of weight	MgO	nil
Al ₂ O ₃	17.10% " "	BaO	nil
Fe ₂ O ₃	traces	K ₂ O	13.98%
CaO	nil	Na ₂ O	1.36%.

Stechiometric calculations on the above analysis showed that the content of orthoclase particles was 82.41%, that of albite particles 11.53%, the remainder being quartz concealed in grains of the mixture and indiscernible under the microscope.

This analysis is very significant, for the total lack of BaO and CaO proves that there were no celsian or anorthite present. Spherulites, which constituted 50% of the analysed mixture and which were analysed together with sanidine, in the end gave uniform results. The mixture was therefore equivalent in its chemical composition to that of potash feldspar with 15% albite particles.

However, spherulites having the same composition as sanidine, were distinguished by their high refraction index. In the literature that was available we did not find any mention of a mineral having the characteristics observed microscopically in spherulites. Hence the deduction that these spherulites belong to some hitherto unknown form of potassium minerals, chemically identical with sanidine and orthoclase, but optically differing from them considerably. In our case we might explain their origin by thermal action. It might, for instance, have taken place during some phase of the evolution of volcanic action in the region of Cracow. A secondary »overheating« of trachytes and tuffs (genetically coupled with them) may have occurred and this may have been the cause of the metamorphism of a considerable part of the sanidines into spherulites with a »condensed« structure.

The structural »defects« of primary sanidine having been thus regenerated, they may have obtained a higher index of light refraction in the newly created elements (the spherulites), without any significant change of specific weight. We believe that a rise in temperature of 600 to 900 degrees would have been sufficient to effect this.

The Appearance of Peculiar Polymerism among Hydrated Alumino-Trisilicate Calcium Minerals

by

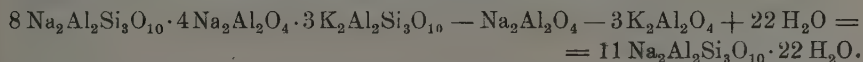
S. J. THUGUTT

Communicated at the meeting of March 16, 1953

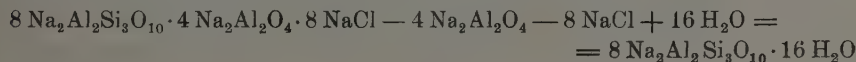
As soon as it appeared that the phenomenon of peculiar polymerism in regard to the reiteration of the link $\text{Na}_2\text{Al}_2\text{Si}_3\text{O}_{10} \cdot 2\text{H}_2\text{O}$ [1] occurred between monoclinic natrolite and rhombic epinatrolite [7], it was to be expected that similar relations also occurred between the calcic substitution products of both minerals. Indeed, besides monoclinic scolecite, which has been known for a long time, a calcic equivalent of sodic epinatrolite was discovered by H. Michel [2] and called (perhaps not quite suitably), meta-scolecite. For in this case we have to deal with a peculiar polymeric and not an isomeric body, to which points the reiteration of the link $\text{CaAl}_2\text{Si}_3\text{O}_{10} \cdot 3\text{H}_2\text{O}$, as it is indicated among others also by the specific gravity of both these minerals:

the higher one for scolecite	$11 \text{ CaAl}_2\text{Si}_3\text{O}_{10} \cdot 33 \text{ H}_2\text{O}$,
the lower one for episcolecite	$8 \text{ CaAl}_2\text{Si}_3\text{O}_{10} \cdot 24 \text{ H}_2\text{O}$.

With this in view, the author used the rule of G. Bischof [3], stating for pseudomorphs the connection between the paternal mineral and its transformation product. Supposing that the transformation was accomplished without change of volume, Bischof concluded that the molecular relation of the paternal mineral and the product obtained must correspond to the ratio of their specific gravities. Concerning nephelite and natrolite, this ratio is $4536 : 4180 = 2.64239$, based on the constitution formula of nephelite [4]:



Concerning sodalite and epinatrolite this ratio is $3876 : 3040 = 2.34 : 1.835$, grounded on the constitution formula of sodalite [5]:



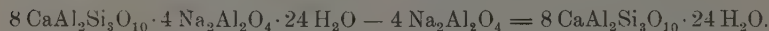
The specific gravities of monoclinic natrolite are all in all conformable with the above figures. Concerning the specific gravity of rhombic epinatrolite, these figures are too high for reason of its frequent coalescence with monoclinic natrolite.

At last it behoves to mention that the double shape of hydrated aluminotrisilicic sodium was first detected by W. C. Brögger [6], without his realizing the cause of this double form.

Both minerals, scolecite and episcolecite, have fully preserved the symmetry of their paternal minerals. Even the hemiedry of natrolite found its repetition in scolecite. The same concerns its pyro-electric properties. Scolecite, when heated, becomes polar electric. One third part of the water contained therein volatilizes more easily than the remaining two thirds. The double refraction is 0.007. The specific gravity is uncertain: 2.274 to 2.31, which is caused by impurities. $n_\alpha = 1.509$, $n_\beta = 1.515$.

Episcolecite found at Olawa (Eulau in German) in marl, in contact with phonolitic rock, shows a weaker double refraction than scolecite and a much lower specific gravity: 2.195. $n_\alpha = 1.504$, $n_\gamma = 1.508$. The paternal mineral of episcolecite is epinatrolite, appearing in phonolite ground as a transformation product of sodalite or noseite. Epinatrolite, when carried away by water in a dispersed condition, collects little by little in neighbouring marl and there exchanges its sodium ions for the calcium ions which attack it on all sides, without losing its proper degree of symmetry during the process.

Scolecite and episcolecite are secondary products and as such belong to the younger generation of zeolites. Thomsonite is closely associated and may also serve, besides epinatrolite, as a source of episcolecite. This transformation into episcolecite is accompanied by the loss of the aluminate link $4\text{Na}_2\text{Al}_2\text{O}_4$, which is very sensitive to the agency of water.



REFERENCES

- [1] Thugutt S. J., Rozprawy Wydz. Mat.-Przyr., Pols. Akad. Um. A. **74** (1949), N 2.
- [2] Michel H., Z. f. Krist. **57** (1922), 672.
- [3] Bischof G., Lehrb. d. chem. u. phys. Geologie **2** (1851), 266 Th. 1.
- [4] Thugutt S. J., N. J. f. Min. Beil.-Bd. **9** (1895), 588.
- [5] Thugutt S. J., Ib. 570.
- [6] Brögger W. C., Z. f. Krist. **16** (1890), 609 u. 622.
- [7] Thugutt S. J., C. R. Soc. Sc. de Varsovie, Cl. III **42** (1949), 146.

A Hydrodynamical Theory of the Origin of Pegmatite Veins

by

S. J. THUGUTT

Communicated at the meeting of January 12, 1953

The origin of pegmatite veins has not yet been sufficiently elucidated in spite of many-sided attempts in this field. Pegmatite veins are extremely complicated bodies, including, according to A. Fersmann [1], some 250 minerals of which 50 are especially typical. Formerly a magmatic and later an aqueous origin was ascribed to pegmatite veins. Recently attempts have been made to combine both these conceptions: it was assumed that the hydrothermal stage was preceded by magmatic action. As this theory lacked any experimental foundation, the structure itself of the veins was taken as a base. The American scientists, E. N. Cameron, R. H. Jahns, A. H. M. Mac Nair and L. R. Page [2] are the greatest contributors to the study of this problem. Their paper contains ample and valuable material pertaining exclusively to the United States of America. The following structural units were determined among pegmatite bodies: fissural fillings, metasomatic formations and concentric zones surrounding a core. It was ascertained that streaks of the external part of the veins were fine-grained, while the adjoining central zones had a coarse-grained structure, containing many minerals, sometimes attaining gigantic crystal sizes. The core of the veins was filled with quartz, often with an admixture of microcline. Among the minerals of the external part were: potash feldspar, muscovite and quartz, as well as accessories such as: tourmaline, apatite, beryl and garnet. In the central zone the presence was ascertained of: microcline, plagioclase, biotite, perthite, graphic granite and clevelandite. The sequence of association of mineral components proved to be significant. Metasomatic phenomena could be recognized chiefly owing to pseudomorphoses that were very often of an original character.

The American authors as well as A. Fersmann examined the three theories of the origin of pegmatite veins, namely: crystallization of magma in situ, crystallization from aqueous solutions, and joint occurrence of both genetic types. Of these they chose the third possibility. A lack of contact

transformations in the surrounding rock speaks against the magmatic origin. Nor is it possible to understand lenticular forms, veins wedging out at both ends, vacuums or fissures not filled by rock material, limestone xenoliths not affected by magma, etc. Assuming hydrogenesis, various authors considered that crystallization could take place either in an open or in a closed environment. In the first case we should expect an increase of anortite content in the plagioclase in the direction of the vein's axis. This is, however, not the case, and a closed environment seems more probable. But here, too, there is no known reason why small-grained components should prevail in the external part of the vein, while large crystals sometimes grow in the central zone; or why a radiate structure or one-sided crystal efflorescences should appear. These and other doubts cannot be explained by any existing theory except by the hydrodynamical theory of liquid veins, which we applied [3] to the Tatra pegmatites investigated by W. Pawlica and considered by him as typical magmatic products.

If a liquid (coloured for that purpose) penetrates with varying velocity by a small opening of 2.45 millimetres in diameter, into an environment filled with a different liquid, there occurs the phenomenon of "liquid veins", known in hydromechanics. Marian Smoluchowski [4] has shown that this is the result of the coaction of inertia and viscosity. The formation of out-flow veins occurs even at the very small velocity of 0.5 cm/sec. and the velocity along the vein axis is comparatively greater, while decreasing towards the walls. As the inflow velocity rises, there is a continuous change

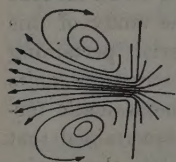


Fig. 1

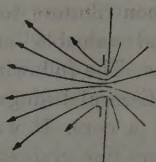


Fig. 2

in form of the current lines. The asymmetry increases with the speed, while the form of the stream corresponding to the smallest velocity is nearly symmetrical. This gradual disappearance of symmetry of the current lines and the gradual incurvation of the streams that flow into the vein with increasing velocity, is clearly visible in Figs. 1 and 2, which illustrate

speeds of 0.9 and 0.45 cm/sec. It is noteworthy that whirlpool rings form behind the opening (see Fig. 1). The surrounding liquid also takes part in the movement of the vein, though less strongly.

As regards pegmatite veins, these whirlpool rings — appearing on the boundary of the vein, but at some distance from this boundary — are specially favourable areas for the formation of crystallization centres and providing them with new material from all possible directions. It is here that the great crystals are formed, single or multiple, in associations called perthites or graphic granites, depending on the nature of the minerals growing in parallel position. On the boundary of the whirlpool ring and interrupted rock the quick flow of liquid causes the crystallization of small-grained material. At a reduced velocity of the stream, no more whirlpools

form; the current deflects sidewise, carrying material specially inclined to form radiate crystals, which grow from the periphery towards the centre of the vein. In these conditions radiate hemispheres arise, formed by needles of tourmaline or andalusite, grouped harmoniously on the margin of the vein. The final stage is marked by an orderless deposition of the contents as the velocity of the current increases. Small-grained bodies, such as are observed in aplite veins are formed.

If we place the opening, introducing the liquid in Smoluchowski's experiment, at the side instead of in the middle of the top wall, the current follows another direction. Instead of concentric forms, one-sided ones appear. Any inflections or juts of the walls will complicate the image still further. And, since such irregularities are to be expected in nature in endless combinations, the schema described above cannot be applied to all cases.

REFERENCES

- [1] Fersmann A., *Min. Petr. Mitt. N. F.*, **41** (1931), 64.
- [2] Cameron E. N., Jahns R. H., MacNair A. H. and Page L. R., *Econ. Geol.*, **40** (1945), 588.
- [3] Thugutt S. J., *Arch. de Minéral. de la Soc. Sci. de Varsovie*, **1** (1925), 59.
- [4] Smoluchowski M., *Sur la formation des veines d'efflux dans les liquides*, *Bull. Intern de l'Acad., des Sci. de Crac. Cl. des Sci. Math.-Nat.* **8** (1904), 371—384.

